Angle-resolved photoemission study of the α-Sn/CdTe(100) interface

Ming Tang and David W. Niles
Synchrotron Radiation Center, University of Wisconsin–Madison, 3731 Schneider Drive, Route 4, Stoughton, Wisconsin 53589-3098 and Department of Physics, University of Wisconsin–Madison, Madison, Wisconsin 53706

Isaac Hernández-Calderón
Departamento de Física, Centro de Investigación y Estudios Avanzados del Instituto Politécnico Nacional, Apartado Postal 14-740, 07000 México, Distrito Federal, Mexico

Hartmut Höchst*
Synchrotron Radiation Center, University of Wisconsin–Madison, 3731 Schneider Drive, Route 4, Stoughton, Wisconsin 53589-3098
(Received 29 December 1986)

We studied the growth of diamond structured Sn on CdTe(100) by angle-resolved photoemission spectroscopy with synchrotron radiation in the photon-energy range $h\nu = 12-34$ eV. Sn grows layer by layer in the α phase on CdTe(100). The α-Sn/CdTe(100) interface is abrupt and nonreactive. We observe neither outdiffusion nor segregation of Cd in the α-Sn layer. A Schottky barrier of $V_{SB} = 0.55$ eV develops after the adsorption of $\frac{1}{4}$ monolayer of α-Sn on p-type CdTe(100).

I. INTRODUCTION

The performance of modern semiconducting devices such as modulation-doped heterostructure lasers and detectors depends critically on the interfacial properties of the constituents semiconductors. The new effective-mass filter (EMF) photodetector, for instance, consists of several hundred alternating layers of $Ga_{1-x}In_xAs$ and $Ga_{1-x}Al_xAs$. Each layer measures about 5 crystal units thick and maintains its quantum size effect only if the interfaces between the two materials are atomically flat, ordered, and abrupt. Unfortunately systems which form a nonreactive stable interface with two-dimensional growth and without intermixing, segregation, or clustering are rare.

The α-Sn/CdTe superlattice is a potential heterostructure laser candidate with interesting electronic properties. The confinement of a thin α-Sn layer between CdTe (band gap $E_g = 1.56$ eV at 300 K) opens the symmetry-induced zero gap band of α-Sn and splits it into two-dimensional sub-bands in the direction normal to the layers.[1] A layer-thickness dependent energy gap appears between the extrema of the lowest valence and highest conduction band. Recent theoretical examinations of the quantum size effect of α-Sn by Craig and Garisson[1] show that a maximum band gap of $E_g \sim 430$ meV results for a film thickness of 40 Å. Other calculations considering the dielectric response of thin α-Sn indicate that the typical bulk singularities in q^{-1} and $w^{-1/2}$ are not present in a thin film.[2] The static dielectric constant depends linearly on the α-Sn film thickness. Due to a gap-independent effective mass and a drastic change in the joint density of states, the absorption coefficient of a thin α-Sn film is much higher and more abrupt than that of an alloy semiconductor with a comparable energy gap.

From a theoretical standpoint, α-Sn/CdTe is a promising heterostructure, but can we actually make a working superlattice from α-Sn and CdTe? These materials present two problems: Sn is stable at room temperature in the β phase, not in the α phase,[3] and CdTe has an unstable surface which frequently leads to Cd diffusion into an adjacent material.[4–6] Substrate interaction with the epilayer in the form of self-doping, and diffusion or interface alloying can change or ruin the performance of a superlattice system completely. Since the expected energy gap in the α-Sn film is small it is particularly sensitive to the degree of spatial quantization of its conduction-band electrons, and therefore to the interfacial properties. A useful superstructure requires a stable α-Sn and an atomically flat and sharp junction between it and CdTe. Fortunately, the nearly perfect lattice match between α-Sn and CdTe solves both of these problems.

Recent experiments demonstrate the ability to grow high-quality α-Sn films by heteroepitaxy on InSb and CdTe surfaces.[7–11] The diamond structured α-Sn grows in registry with the zinc-blende structure of the substrate. The small lattice mismatch of $<0.14\%$ favors two-dimensional growth and gives rise to a nearly strain-free ideal interface region. Raman experiments studying the phase transition from the semiconducting α phase into the metallic β phase show that the substrate interfacial bonds act to stabilize the phase transition.[12] Thin α-Sn films grown on InSb(100) transform into the β phase at ~ 115 °C whereas the transition temperature for bulk α-Sn crystals occurs well below room temperature at ~ 13.2 °C. The increased thermal stability of thin α-Sn films may allow the growth of CdTe layers by MBE at moderate temperatures on top of α-Sn.

The Cd diffusion problem may be solvable as well. Previous experiments with various metal overlayers on CdTe show that the interfaces are usually not atomically abrupt. Among all of the III-V and II-VI compounds studied, CdTe has one of the most unstable surfaces.[4–6]

Several metal monolayers are necessary to build the Schottky barrier and to produce the maximum surface Fermi level shift. In contrast, GaAs needs only fractions of monolayer to develop fully the Schottky barrier.[5,13,14] Brillson observed a relationship between the interface reactivity, the Schottky-barrier height, and the heat of reaction.[15] He found that most reactive metals, those with negative heats of reaction, formed abrupt interfaces and low Schottky barriers whereas unreactive metals, those with positive heat of reactions, developed wide interfaces and high Schottky barriers. The heat of reaction for Sn to form a SnTe compound is $+0.33$ eV/metal-atom.[6] This value is just slightly higher than the necessary critical value of 0.3 eV/metal-atom needed to make a Schottky barrier.

The aim of the present paper is to investigate the interface formation and the epitaxial growth of α-Sn on CdTe(100) in order to provide important parameters such as the Schottky-barrier height, the interface width, and the interfacial composition. Since these parameters critically determine the effectiveness of an α-Sn/CdTe superstructure used as a sensitive high-speed detector, a detailed study of them is a necessary prerequisite to the successful MBE growth of the superlattice structure. We have used angular-resolved photoemission spectroscopy with synchrotron radiation as a local microscopic probe to investigate the CdTe(100) surface properties and the α-Sn interface formation. Based on Sn and Cd 4*d* core level spectra, we find that Sn does not react with the substrate and Cd does not diffuse through the Sn layer. Valence-band and core level spectra clearly indicate the growth of semiconducting α-Sn. The interface region is fairly abrupt. A thin film of $\frac{1}{4}$ monolayer saturates the band bending and pins the Fermi level at ~ 0.55 eV above the valence-band maximum.

II. EXPERIMENTAL

Mechanical polishing brought crystal plates of 8×8 mm^2 and about 1-mm thickness of *p*-type CdTe oriented with the [100] axis perpendicular to the face to a mirror finish. Simultaneous sputtering with Ar ions of 500-eV energy and mild annealing to ~ 270 °C removed surface contamination and crystal damage left by the cutting and polishing. Obtaining a clean and well-ordered surface required sputtering and annealing for more than 10 h. The diffraction pattern from low-energy electron diffraction (LEED) showed sharp spots. CdTe(100) surfaces annealed at 400 °C exhibit a one domain (2×1) reconstruction.[16]

A liquid-nitrogen shielded molecular beam cell equipped with a high-purity carbon crucible provided the Sn films. At cell temperatures of ~ 1200 °C the typical growth rate was ~ 1 Å/s. We monitored the evaporation rate with a thermally stabilized calibrated quartz thickness monitor. During the growth the sample was held at room temperature.

We performed the angle-resolved photoemission experiments at the University of Wisconsin–Madison electron storage ring in Stoughton, Wisconsin using photons in the range $h\nu = 12-34$ collected from a Seya-Namioka type monochromator. The total angular acceptance of the hemispherical sector analyzer was $\sim 2°$. The total energy resolution of the spectrometer-monochromator unit was ~ 200 meV, as determined from the measured width of the Fermi edge of metallic Sn. The angle of incidence of the photons was 45° with respect to the surface normal. To measure work function changes, $\Delta\Phi$, induced by the Sn overlayers, we biased the sample with a negative potential and extrapolated the cutoff energy of the secondary electrons in the photoemission spectra. The errors for the relative measurements of $\Delta\Phi$ are ~ 20 meV.

III. RESULTS AND DISCUSSION

A. Cd 4*d* core level spectra

Figure 1 shows the Cd 4*d* core level spectra measured with $h\nu = 22$ eV of clean and Sn-covered CdTe(100) taken under normal emission. The binding energies for the Cd $4d_{3/2,5/2}$ levels are at 10.86 and 11.45 eV, respectively. These results agree with those of previous experiments.[6] Recent work by John *et al.*,[16] however, showed additional structure in the Cd 4*d* spectra which they assigned to two surface shifted components. One component represented the surface Cd which is bound to Te while the other one indicated free Cd on the surface. In previous experiments we produced similar multicomponent core level spectra with different relative intensities by annealing to temperatures above ~ 300 °C. Since the present experiment addresses the problem of metastable phase heteroepitaxy, we avoided the diffusion of Cd to the surface by annealing only to 270 °C. Cd 4*d* spectra taken with higher surface sensitivity at $h\nu = 32$ eV showed also only a single spin orbit doublet whereas John *et al.*[16] reported an additional surface sensitive structure having $\sim 30\%$ of the intensity of the bulk spectrum.

Deposition of Sn shifts the Cd 4*d* spectra by ~ 0.24 eV towards higher binding energies. This binding energy shift reflects a downward band bending induced by the Sn atoms of initially flat bands. The opposite situation where the clean CdTe surface originally has bent bands which are flattened by the addition of Sn cannot be the case here, since an initial band bending of the clean surface would necessarily place the bulk Fermi level close to the midgap position of 0.60 eV above the valence-band maximum (VBM). The CdTe substrate used in this experiment is highly *p* type with the Fermi level in the bulk close to the valence-band maximum. Additional coverage beyond 0.25 monolayers (ML) produces no further band bending which indicates a pinned Fermi level and a sharp interface with two-dimensional layer growth. A clustered overlayer growth as seen, for example, with Ag on GaAs(110) shows a shift of the valence band extending over several monolayers.[17]

Analysis of the attenuation of a substrate core level with increasing overlayer thickness gives more direct proof of the growth mode. For a two-dimensional layer by layer growth the substrate core level intensity reduces exponentially as $I = I_0 \exp(-d/\lambda)$ where d is the overlayer film thickness and λ is the characteristic electron mean free path in the overlayer material. Figure 2 shows the intensity decrease of the Cd 4*d* core emission

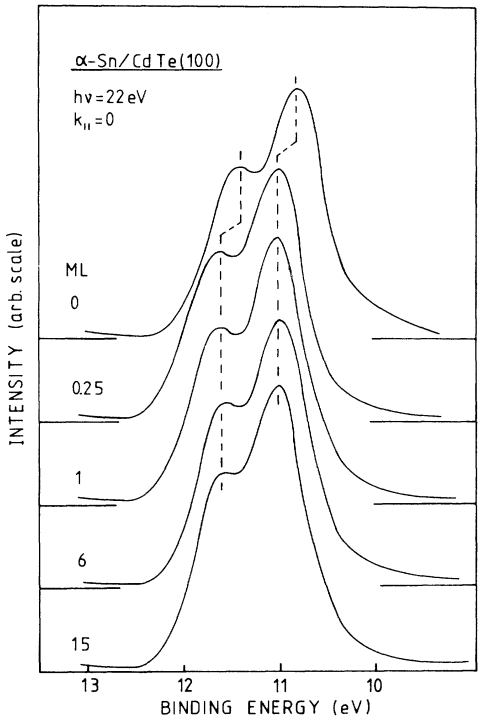

FIG. 1. Cd 4*d* core level spectra as a function of α-Sn(100) coverage. All spectra have been taken with $h\nu=22$ eV at normal emission. (ML represents monolayer.)

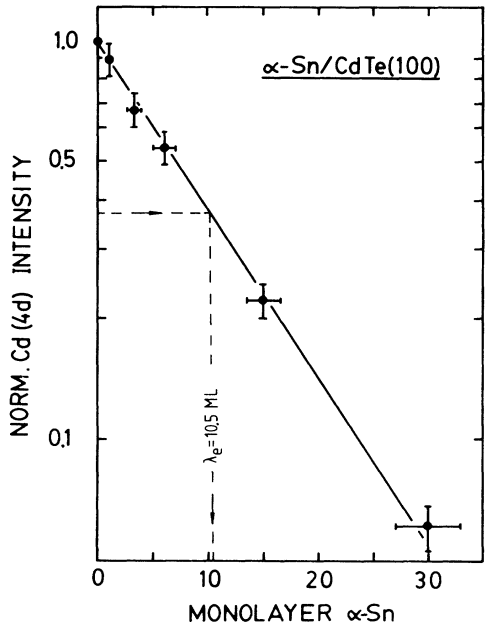

FIG. 2. Decrease of Cd 4*d* core level emission as a function of α-Sn coverage.

as a function of α-Sn monolayers. The data points follow perfectly the exponential attentuation equation $\ln(I/I_0)=-d/\lambda$. The observed exponential decrease of the Cd 4*d* intensity (normalized to the zero coverage intensity) with increasing Sn coverage provides strong evidence for an abrupt two-dimensional layer growth of Sn. Out diffusion of free Cd through the overlayer observed for numerous metal/CdTe interfaces does not occur at the α-Sn/CdT(100) interface.

The exponential substrate attenuation allows also the determination of the electron escape depth. An attenuation of the Cd 4*d* intensity by $1/e$ occurs at an overlayer coverage equal to the mean free path. From Fig. 2 we deduce a mean free path of $\lambda=10.5$ ML of Sn, or $\lambda=17$ Å for electrons with $\sim$6-eV kinetic energy. Accurate electron mean-free-path values are still scarce in the literature for semiconductors. This scarcity is particularly true for the low-energy side of the escape depth function. Our value of $\lambda=17$ Å agrees reasonably well with those obtained for Si, Ge, and GaAs measured in the same kinetic energy region.[18–20]

B. Valence-band spectra

Figure 3 shows the evolution of the α-Sn valence-band spectra as a function of the Sn coverage taken at normal emission with $h\nu=20$-eV photons. The angular-resolved valence-band spectra for the clean CdTe(100) shows in this energy range a typical three peak structure. The peaks labeled *A* and *B* at $\sim$2.0 and $\sim$3.4 eV binding energy which disperse with photon energy originate from

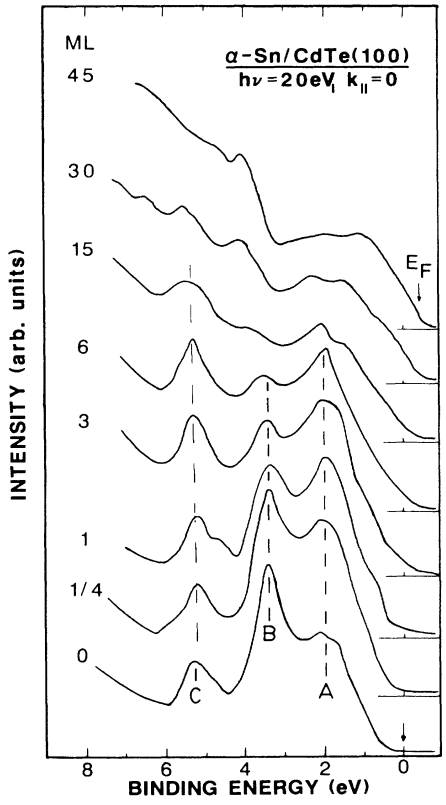

FIG. 3. Normal emission valence-band spectra of the α-Sn/CdTe(100) interface as a function of α-Sn coverage. The Fermi level of the α-Sn-covered samples has been shifted according to the binding-energy change of the Cd 4*d* core level.

direct transitions out of the first and the second bulk valence bands of CdTe. (The dispersion with photon energy is not shown in the figure.) The third peak C which does not disperse with photon-energy results from indirect transitions with initial states at flat band regions ($\partial E/\partial k=0$) near the X and K points.[21] Indirect transitions from these regions are very typical for materials with zinc-blende structure. The relatively high intensity does not necessarily imply that the material is of bad single-crystal quality, but rather reflects mainly the existence of a large volume in k space with a high density of states due to flat regions of the valence bands.

The characteristic CdTe(100) valence-band spectrum diminishes gradually with increasing Sn coverage. Direct transitions are extremely sensitive to overlayer adsorption, since they represent the initial-band structure at a particular k point. The indirect transitions, conversely, are an integral measure of the band structure over an extended k range and are much less sensitive to the presence of the adsorbed overlayer. As one observes, from Fig. 3, the heights of peaks A and B immediately change with small amounts of Sn and finally their relative intensities reverse. Peak C, on the contrary, remains nearly uneffected for small coverages. As deduced from the Cd 4d core level binding-energy shift (see Fig. 1), the adsorption of Sn produces an interface dipole which forces a downward bending of both the CdTe bands and the Cd 4d core level at the interface region. Correcting the band bending effect by shifting the valence-band photoemission spectra by the same amount towards lower binding energies realigns the characteristic emission structures with features of the clean CdTe(100) surface.

From a first glance this figure gives the impression that the interface evolves over a region of ~ 20 ML in thickness. However, determining the interface width by following the decay of the substrate valence-band emission and the evolution of the overlayer emission in a binding-energy region where both materials contribute to the spectra is very difficult. Attenuating the underlying substrate emission so that the unperturbed overlayer spectrum is detectable requires an overlayer thickness well above the photoelectron escape depth λ. From Fig. 2 we determine the escape depth $\lambda \sim 10$ ML for electrons of $E_{\rm kin} \sim 6$ eV. For valence-band electrons excited with $h\nu=20$ eV the kinetic energy is slightly higher and therefore the escape depth is somewhat smaller. By comparison with the mean free path in Si (Ref. 18) we estimate a mean value of the escape depth $\bar{\lambda} \sim 8$ ML for the valence-band region in α-Sn.

Keeping in mind that the intensity of an electron beam passing through a layer of thickness λ attenuates by 64% and that of a layer of thickness of 3λ by 95%, we see that even for an atomically abrupt interface the valence-band photoemission spectrum has to show noticeable changes over a film thickness of at least 2λ. Thus the apparent change in the valence bands shown in Fig. 3 over a 15-ML thickness is exactly what is expected from a sharp interface.

The emission increase around the Fermi level with increasing Sn coverage is more clearly visible in Fig. 4 where spectra are taken at $h\nu=20$ eV and $\Theta=23°$ off

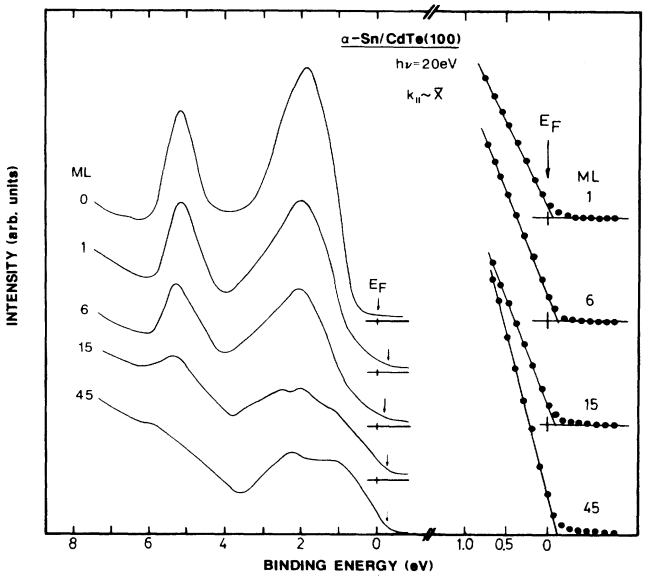

FIG. 4. Valence-band photoemission spectra of the α-Sn/CdTe(100) interface taken around the boundary of the surface Brillouin zone at the $\bar{X}$ point.

normal. The parallel component $k_{\parallel}$ of the outcoming photoelectron points along the [110] direction. For electrons with a binding energy of a few eV and a work function $\Phi=4.36$ eV for the α-Sn(100) the $k_{\parallel}$ component is around the $\bar{X}$ point of the first surface Brillouin zone. Around this region in **k** space the top of the valence band is dispersed further away from E_F, and bands responsible for peaks A and B in the normal emission spectra of Fig. 3 move closer together. By dispersing the substrate valence-band emission towards higher binding energy the emission from the Sn overlayer becomes dominant near E_F. We will present a more detailed analysis of the CdTe experimental band structure along high-symmetry lines in **k** space and around characteristic **k** points in the surface Brillouin zone in a separate paper.[22] For the present study the important observation is that the valence-band spectra at $\sim\bar{X}$ exhibit less structure than those taken with $\mathbf{k}_{\parallel}=\mathbf{0}$ at $\bar{\Gamma}$.

The reduction to only two main features in the substrate valence-band spectra makes the detection of new α-Sn–related structures much easier. As seen in Fig. 4 the adsorption of small amounts of Sn causes again an immediate increase of emission in the CdTe gap region below E_F and a subsequent reduction of the two characteristic CdTe peaks. The right part of Fig. 4 shows an enlarged part of the region ~ 1 eV below E_F. These spectra which were produced by a difference curve between the Sn covered and the clean surface show that the photoemission intensity from a 1-ML α-Sn overlayer and a thick α-Sn film both fall linearly and intersect the abscissa at the Fermi level. The only difference between the thin and the thick films is that the total intensity in this energy region for thicker films leads to a steeper slope of the difference spectrum. Additional Sn beyond 1 ML simply adds to the existing Sn emission but does not produce additional features.

The immediate "pinning" of the leading edge of the valence-band spectra close to E_F is strong evidence for an abrupt interface between CdTe(100) and the ordered overlayer growth of α-Sn. Near E_F we see neither the formation of interface gap states nor the evolution of thickness-dependent occupied quantum-well states. Metallic Ag overlayers on Si show clearly these thin film related states.[23] Recent calculations employing the linear combination of atomic orbitals (LCAO) method confirm the existence of one-dimensional quantum-well states for the α-Sn/CdTe(111) interface.[1]

The truncation of the number of α-Sn layers leads to a strong perturbation of the p orbitals which are oriented along the [111] direction. The binding energy of the p-like bonding orbitals varies slowly from ~ 100 meV below E_F for a 30-Å thick film and approaches E_F at an overlayer thickness of ~ 100 Å. The antibonding p-like conduction band state shows a slightly different thickness dependence. For 20 Å of α-Sn it starts at ~ 180 meV above E_F, reaches a maximum of ~ 320 meV at 40 Å, and comes back to about 100 meV above E_F for 100 Å of α-Sn. Unfortunately, theorists have performed calculations only along the [111] direction. The properties of the bonding and antibonding orbitals in a thin layer confined along the [100] direction is, therefore, not clear. The shape of the inelastic scattered electron tail in low-energy electron loss experiments seem to verify the existence of empty (conduction-band) quantum-well states for this system.[24] Despite the evidence in favor of gap states, the results here neither prove nor disprove their existence.

These experiments do not provide evidence of a sharp localized thickness-dependent emission in the energy range ~ 1 eV below E_F. At present, though, we can not rule out the existence of quantum-well related valence-band states for α-Sn/CdTe(100) interface. The total experimental energy resolution of $\Delta E \sim 200$ meV may smear narrow structures. Cross sections or symmetry rules may lower or even forbid transitions for the present detection geometry. More theoretical and experimental work is needed in order to enhance the detection efficiency of the expected quantized conduction states by either tuning the photon energy or searching with different excitation geometries in other areas in the Brillouin zone.

C. Sn 4*d* core level spectra

Figure 5 shows the evolution of the Sn 4d core level spectra with increasing Sn coverage, taken under normal emission with $h\nu = 34$ eV. The binding energy of the Sn $4d_{5/2}$ level is at 23.8 ± 0.05 eV for small coverages of α-Sn and it shifts continuously with increasing coverage to 23.95 ± 0.05 eV for 45 ML of Sn. The binding energy for a bulk film of the metallic β-Sn (as shown in the top of Fig. 5) is ~ 150 meV smaller than that of a bulk α-Sn sample. Friedman *et al.*[25] predicted a shift towards smaller binding energies for the Sn 4d levels in β-Sn but their calculated absolute value of $\Delta E_B(4d) = 0.3$ eV is much bigger than what we found. Friedman *et al.*[25] also performed an experiment to measure the binding-energy difference between the 4d levels of α- and β-Sn. By cooling a polycrystalline β-Sn sample, they found a shift of $\Delta E_b(4d) \sim 0.32$ eV. However, the applicability of their observed shift to the formation of α-Sn at temperatures below 13.2 °C is not clear at this point since they did not report the disappearance of a strong Fermi level emission of the metallic β phase after the phase transition nor did they do any other additional studies to verify the α-phase formation after the sample was cooled down for a sufficiently long time.

The small increase in binding energy of the Sn 4d level with increasing α-Sn coverage could result from the interface dipole layer. The downward band bending of the p-type CdTe after the adsorption of Sn creates a positive charge accumulation at the Sn interface while the negative charge distribution decays into the CdTe substrate. The decay length depends mainly on the carrier concentration and extends in a semiconductor typically over several 100–1000 Å.[26] On the metallic side of the barrier the decay length is usually sufficiently short. The first layer screens the charge causing the bending. In the present case where the Sn overlayer grows as s semimetal thin film or as a small gap semiconductor, one may also expect a fairly short decay of the band bending over several layers on the Sn side of the interface.

In addition to a shift in binding energy between the two Sn phases, the Sn 4d emission is $\sim 50\%$ broader in the α phase than in the metallic β phase. The small (~ 150

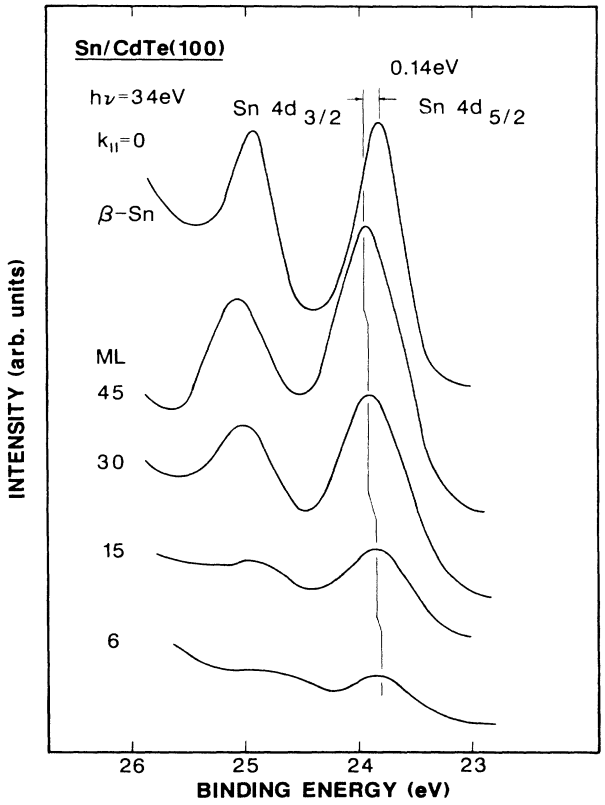

FIG. 5. Photoemission spectra of the Sn 4d core level of the α-Sn/CdTe(100) interface as a function of Sn coverage. The spectra have been measured under normal emission with $h\nu = 34$-eV photons.

meV) band bending in the Sn overlayer could cause these broadenings. For a decay length of the band bending comparable with the mean free path of the photoelectrons, the spectra is a superposition of transitions with different binding energies.

General inhomogenities and Sn cluster formation cannot be the source of the broadening since the Sn film grows layer by layer. The small lattice mismatch of 0.14% with the CdTe substrate, however, causes some strain which may effect the electronic structure over an extended film thickness. We have begun additional quantitative studies of strained α-Sn epilayers which may shed some more light on this aspect. At this point we can only speculate about the origin at the small binding-energy shift and increased peak width of the Sn 4*d* emission in α-Sn.

D. Energy-level diagram of the α-Sn/CdTe(100) interface

Photoemission spectroscopy provides an excellent tool for extracting from one experiment important interface parameters such as band offsets ΔE_{VB}, positions of E_F with respect to the top of the valence band and electron affinities χ. Figure 6 shows the Cd 4*d* and Sn 4*d* binding-energies shifts, the Schottky-barrier formation in the valence band, and the work function changes with increasing α-Sn coverage. We reference all energies with respect to the Fermi level which remains constant throughout the interface. Using this energy presentation causes the vacuum level VL to follow the changes $\Delta\phi$ of the work function. We have measured the work function from the photoemission spectra around the photoemission threshold region. Biasing the sample allowed clear distinction between the different work functions of the sample and the electron analyzer. The absolute accuracy of the work function Φ is ~200 meV and reflects the accumulation of errors in determining the photon energy, the Fermi level, the top of the valence-band emission, and the exact point of the photoemission cutoff. The relative change of the work function $\Delta\phi$, however, is much more accurate. The estimated error for $\Delta\phi$ is ~20 meV. As seen in Fig. 6 the deposition of Sn lowers the photoelectric threshold from the CdTe(100) value of $\phi=5.26$ eV to the thick α-Sn value of $\phi=4.35$ eV.

The work function change is not abrupt during the interface growth. Initially it decreases sharply by $\Delta\phi\simeq 0.21$ eV for 0.25 ML of α-Sn but it then slowly changes over the next ~20 ML before reaching the final thickness independent work of bulk α-Sn.

In theory the work function consists of two different contributions. The bulk chemical potential $\bar{\mu}$ which is a measure of the Fermi level with respect to the "zero" of the crystal potential, and the dipole barrier D which is a surface term caused by a "spill over" of charges at the crystal/vacuum interface. Calculations of ϕ considering both quantities $\bar{\mu}$ and D agree reasonably well with experimental data from simple metals.[27] The electron density distribution around the vacuum/metal interface which is responsible for this dipole layer formation changes over relatively short distances. The so called Friedel oscillations of the charge distribution towards the inside of the interface has a typical length of $\sim\frac{1}{2}k_F$. This value indicates that a full dipole layer contribution to the work function develops for a typical metal after 1–2 layers which agrees well with existing data of the work function changes for thin alkali-metal films grown on transition-metal surfaces. Lang and Kohn,[28] however, pointed out that the oscillation length critically depends on the density of states at E_F.

Our work function measurements indicate that charge densities may vary over as much as ~20 ML in a semimetallic material like α-Sn. The presence of an electrostatic field generated by the dipole layer at the α-Sn/CdTe interface may provide an additional contribution to broaden the surface dipole layer at the α-Sn/vacuum interface and thus may cause the α-Sn work function to develop gradually over an extended distance from the CdTe surface.

Extrapolation of the leading edge of the valence-band emission to zero is the usual method for determining the top of the valence band from a photoemission spectrum. Interface studies[29] frequently involve this method but its usage requires some precautions. The emission from the top of the valence band originates from a very localized small **k**-space volume around the Γ point and contributes a relatively small amount to the total emission spectrum. The emission from other regions of the bulk Brillouin zone does not, therefore, force the leading edge of the total emission spectrum to point to the valence-band top at the Γ point. This argument is particularly true for an angle-integrated photoemission spectrum which

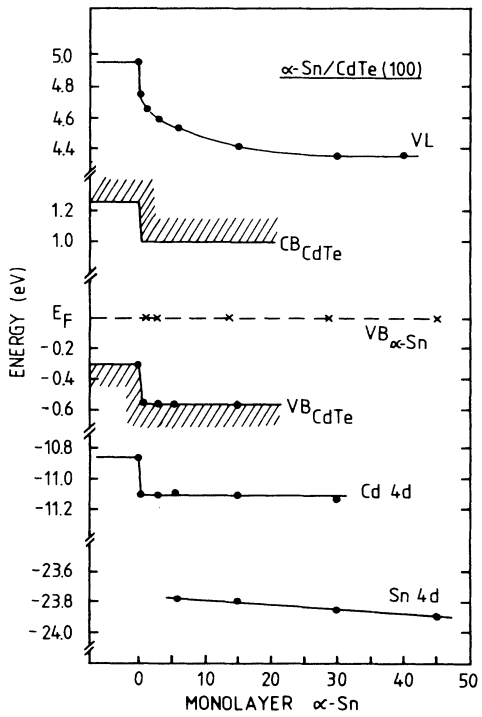

FIG. 6. Evolution of the energy levels of the Sn-CdTe structure as a function of increasing Sn coverage. The shift of the valence band and the substrate core level emission are due to band bending after the deposition of $\sim\frac{1}{4}$ ML of Sn.

must sample over a large part of the Brillouin zone in order to reproduce density of state features. Angle-resolved spectra, on the contrary, sample selectively in **k** space. By changing the photon energy, one tunes transitions along a particular **k** direction and thus allows for a determination of both the binding energy and the **k** vector for a particular feature in a photoemission spectrum. The emission from Γ gives the valence-band top.

We took normal emission spectra of CdTe(100) at different photon energies and determined the emission of the Γ_8 bulk valence band to be 0.3 ± 0.1 eV below the Fermi level. Since the energy gap for CdTe at 300 K is $E_g=1.56$ eV,[30] the bottom of the Γ_6 conduction band lies at 1.26 eV above E_F. Using the experimentally determined photoelectric threshold ($\phi=E_{\rm VL}-E_{\rm VB}$) $\phi=5.26\pm0.2$ eV for CdTe(100) we can also estimate an electron affinity ($\chi=\phi-E_g$) $\chi=3.7\pm0.2$ eV. From photoelectric yield measurements, Swank[31] reported a slightly higher value of $\chi=4.28$ eV.

Adsorption of Sn causes the valence band to bend downward by $\Delta E_{\rm VB}=0.25$ eV with $\frac{1}{4}$ ML of Sn as indicated by the constant binding energy of the Cd $4d$ core level with further Sn coverage. From the 0.25-eV band bending and the separation between the top of the CdTe(100) valence band to E_F we determine a Schottky barrier $V_{\rm SB}=0.55$ eV for the interface of α-Sn with p-type CdTe(100). Applying the Schottky model where the work function difference $V_{\rm SB}=\Phi_S-\Phi_M$ of the two materials determines the barrier height $V_{\rm SB}$ between a metal and a p-type semiconductor, we expect a much higher value of $V_{\rm SB}=0.91$ eV. One frequently observes a discrepancy between experimental and theoretical barrier heights at metal semiconductor interfaces. The shortcoming of the simple model is the presence of interface states which stabilize the Fermi-level shift.

The top of the α-Sn valence band pins at E_F within a coverage of 1 ML of Sn. Angle-resolved valence-band spectra taken around the $\bar{\Gamma}$ and $\bar{X}$ point of the surface Brillouin zone do not give any indication of additional Sn related interface state emission with the onset of the α-Sn/CdTe formation.

IV. CONCLUSIONS

We summarize the angle-resolved valence-band and core level studies of the α-Sn/CdTe(100) interface formation as follows. (i) Sn grows layer by layer in the α phase on CdTe(100) substrates. The α-Sn phase is stable in a thin film well above room temperature (ii) The α-Sn/CdTe(100) interface is abrupt and nonreactive. At room temperature Cd neither interdiffuses nor segregates in noticable amounts on top of the α-Sn films. (iii) α-Sn develops a Schottky barrier with p-type CdTe(100) of $V_{\rm SB}=0.55$ eV.

The encouraging findings demonstrate the possibility of growing a well-defined interface between α-Sn and CdTe. A well-characterized interface is an important precursor to the growth of a high-quality super lattice structure of these two materials. We recently performed additional experiments on the epitaxial growth of CdTe on α-Sn substrates. Core level emission measurements do not give evidence for Cd or Te outdiffusion or Sn_xTe_y compound formation.[32]

ACKNOWLEDGMENTS

This work was sponsored by the Strategic Defense Initiative Organization, Innovative Science and Technology, (SDIO) and managed by the U.S. Naval Research Laboratory (NRL) under Contract No. N00014-86-K-2022. The experiments were performed at the Synchrotron Radiation Center (SRC) of the University of Wisconsin–Madison. The help and friendly assistance of the SRC staff is gratefully acknowledged. One of us (I.H.C.) wants to also thank Centro de Investigación y Estudios Avanzados del Instituto Politécnico Nacional (CINVESTAV-IPN), Mexico, for partial support during his stay in Madison.

*Author to whom all correspondence should be sent.

[1]B. I. Craig and B. J. Garison, Phys. Rev. B **33**, 8130 (1986).
[2]G. A. Broerman, Phys. Rev. Lett. **45**, 747 (1980).
[3]G. A. Busch and R. Kern, *Solid State Physics*, edited by H. Ehrenreich, F. Seitz, and D. Turnbull (Academic, New York, 1961), Vol. 11, p. 1.
[4]C. F. Brucker and L. J. Brillson, J. Vac. Sci. Technol. **18**, 787 (1981).
[5]L. J. Brillson, Surf. Sci. Rep. **2**, 123 (1982).
[6]M. H. Patterson and R. H. Williams, Vacuum **31**, 639 (1981).
[7]R. F. C. Farrow, D. S. Robertson, G. M. Williams, A. G. Cullis, G. R. Jones, I. M. Young, and P. N. J. Dennis, J. Cryst. Growth **54**, 507 (1981).
[8]H. Höchst and I. Hernández-Calderón, Surf. Sci. **126**, 25 (1983).
[9]I. Hernández-Calderón and H. Höchst, Phys. Rev. B **27**, 4961 (1983).
[10]L. Viña, H. Höchst, and M. Cardona, Phys. Rev. B **31**, 958 (1985).
[11]H. Höchst and I. Hernández-Calderón, J. Vac. Sci. Technol. A **3**, 911 (1985).
[12]J. Menéndez and H. Höchst, Thin Solid Films. **111**, 375 (1984).
[13]W. E. Spicer, P. W. Chye, P. R. Skeath, C. Y. Su, and I. Lindau, J. Vac. Sci. Technol. **16**, 1422 (1979).
[14]W. E. Spicer, I. Lindau, P. R. Skeath, C. Y. Su, J. Vac. Sci. Technol. **17**, 1019 (1980).
[15]L. J. Brillson, Phys. Rev. B **18**, 2431 (1978).
[16]P. John, T. Miller T. C. Hsich, A. P. Shapiro, A. L. Wachs, and T. C. Chiang, Phys. Rev. B **34**, 6704 (1986).
[17]R. Ludeke, T. C. Chiang, and T. Miller, J. Vac. Sci. Technol. B **1**, 581 (1983).
[18]H. Gant and W. Mönch, Surf. Sci. **105**, 217 (1981).
[19]D. E. Eastman, T. C. Chiang, P. Heimann, and F. J. Himpsel, Phys. Rev. Lett. **45**, 656 (1980).
[20]I. Lindau and W. E. Spicer, J. Electron. Spectrosc. Relat. Phenom. **3**, 409 (1974).
[21]J. R. Chelikowsky and M. L. Cohen, Phys. Rev. B **14**, 556

(1976).
[22]Ming Tang, D. W. Niles, I. Hernández-Calderón, and H. Höchst (unpublished).
[23]A. L. Wachs, A. P. Shapiro, T. C. Hsich and T. C. Chiang, Phys. Rev. B **33**, 1460 (1986).
[24]S. Takatani and Y. W. Chung, Phys. Rev. B **31**, 2290 (1985).
[25]R. M. Friedman, R. E. Watson, J. Hudis and M. L. Pearlman, Phys. Rev. B **8**, 3569 (1973).
[26]A. G. Milnes and D. L. Feucht, *Heterojunctions and Metal Semiconductor Junctions* (Academic, New York, 1972).
[27]M. Weinert and R. E. Watson, Phys. Rev. B **29**, 3001 (1984).
[28]N. D. Lang and W. Kohn, Phys. Rev. B **3**, 1215 (1971).
[29]See, for example, A. D. Katani, N. G. Stoffel, R. R. Daniels, Te-Xiu Zhao, and G. Margaritondo, J. Vac. Sci. Technol. A **1**, 692 (1983).
[30]S. M. Sze, *Physics of Semiconductor Devices,* 2nd ed. (Wiley, New York, 1981), p. 849.
[31]R. K. Swank, Phys. Rev. **153**, 844 (1967).
[32]Ming Tang, David W. Niles, Elio Colavita, and Hartmut Höchst (unpublished).